COMPARATIVE STUDIES INTO RESONANCE DAMPING OF OUTPUT LCL FILTER FOR ACTIVE POWER FILTER WITH VOLTAGE SOURCE INVERTER

Adjei-Saforo Kwafo Edmund[1,2], Misbawu Adam[1], Samuel Addo Darko[1], Solomon Nchor Akansake[3]

[1]*Faculty of Engineering and Technology, Kumasi Technical University, Kumasi*

[2]*Faculty of Computer and Electrical Engineering, COE, KNUST, Kumasi.*

[3]*Faculty of Physical Sciences Computational Sciences, COS, KNUST, Kumasi.*

Abstract

The active power filters are members of harmonic filtering family which is made up of embedded power electronic devices and it is used for enhancing power quality. However, while addressing harmonic distortion, an overcompensation stemming from step response might occur, leading an extended settling time, thus, driving the system into oscillation. Not all but also, the challenges associated with the control of output LCL filter of APF connected inverter originates from the resonance problem. Therefore, this paper analyses passive damping solutions to suppress the resonance problems of an LCL filter. Six passive damping remedies were considered, according to the location of the damping term. A capacitor with a series resistor, which is widely used is proposed among the six passive damping techniques. The simulations are carried-out using MATLAB/Simulink. The results, compared to others, depict the lowest total harmonic distortion (THD) as well as power loss at the fundamental frequency.

Keywords: *Resonance, Passive damping, Active power filter, LCL filter.*

1.0 INTRODUCTION

In today's world, the transformation occurring in industrial setups is unprecedented owing to utilization of semiconductor-embedded equipment to build a sophisticated variable speed drives and power converters to optimally control range of applications, which has led to enhance production rate. Thus, drivers and power converters have created enabling environment for precision and efficiency control with many applications in a system with various ranges. Additionally, the increase in demand of electricity has resulted an unbearable pressure on the traditional grid calling for integration of renewal energy to augment the system. The essential of this integration system has immensely contributed to reliability and continuous power supply leading to high productivity. Furtherance, the use of the semiconductor -embedded devices placed in the inverters for the renewable energy design cannot be overemphasis. However, the presence of the said devices has introduced a lot of harmonic contamination into the power system thereby affecting the voltage and current waveforms [1-3].

The power quality which is so dependent upon fixed frequency and constant voltage is worthy of consideration since most the loads connected to the grid are very critical, and any variation in the voltage and frequency will consequently affect it operation. In order to mitigate if not to efface these contamination has led to the design and implementation of active power filter (APF) [4,5]. The configuration design has produce different types such as series APF, shunt APF and hybrid APF. They find their applications in low, medium and high voltage transmission level to control the injection harmonic contamination in the power system by the power converters and variable speed drives. The orientational configuration of these passive elements, namely; resistance, inductance and capacitance play an important role in carrying out the filtration of the inverter output current [6-7].

Generally, designing a filter (smoother) for small power system application, a consideration of the system size and rated capacity of the components used are the essential factors. To design and implement conventional filter, is connected to traditional inductance-capacitance or capacitance-inductance filter. The inductance-capacitance-inductance (LCL) smoother has enhanced attenuation and generated reactive output to the point of common coupling of an interactive power system to efface inrush current of the inductance-capacitance smoother. Conversely, the injection of this anti-harmonic current to cancel the system harmonic contamination can lead to over-shoot or undershoot causing the system to oscillate, generating into another harmonic production of different frequencies. Hence, one key factor of smoother design is damping. The active damper which operate in on-line system is quite smarter than the passive damper. In most situations, passive filter is considered as result of its less sophistication connection of the auxiliaries[8-10]. The LCL smoother operation should conform to the requirements of IEEE 519 standards. The challenges associated with the control of output LCL smoother of APF connected inverter arises from the resonance problem. This causes a sharp phase steps down of -180^{O} with high resonance peak at the resonance frequency.

The objective of this paper is to conduct a comprehensive assessment of LCL resonance damping methods. Six different types of passive damping methods, their transfer functions and their Bode diagrams are analyzed and compared by means of resonance attenuation performance and damping losses. MATLAB-Simulink tools are used to verify the performance of the analysis. The challenges associated with the control of output LCL filter of APF connection-inverter arises from the resonance problem. This cause a steep steps down of -180^{O} of with high magnitude of oscillation at the oscillation frequency.

2.0 RESONANCE CHALLENGES ASSOCIATED WITH LCL FILTER

The circuit Figure1(a) depicts the major circuit of a phase LCL output filter of an inverter, and its simplified circuit is shown in Figure 1(b), where L_1 is the inductor in inverter-side, C is the soother capacitor and L_2 is the inductor on the grid side. Figure 2 shows a Bode diagram (BD) of the LCL smoother without damping.

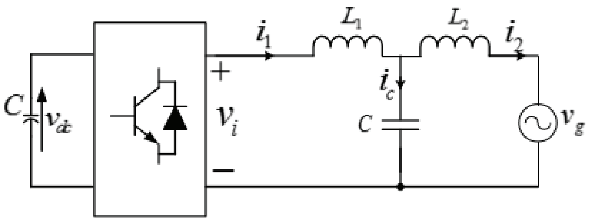

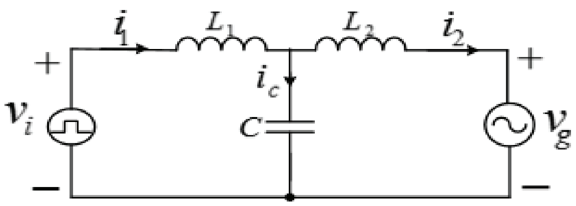

(a) *(b)*

Figure1: A phase LCL smoother connected to grid-interactive system (a) main circuit (b) Generic configuration

From the transfer function, $H_{(S)} = {}^{i_2}\!/_{v_i}$ where the voltage across at the grid system at PCC is assumed perfect source voltage able of deadening all the integral multiple frequencies.

With reference to inverter controlled current and if v_g is assumed zero $(v_g = 0)$, the transfer function can be characterized as follows:

$$i_2 = \frac{i_1}{s^2 L_2 C + 1} \tag{1}$$

$$i_1 = i_2 (s^2 L_2 C + 1) \tag{2}$$

$$v_i = i_1 \left(sL_1 + \frac{sL_2}{s^2 L_2 C + 1} \right) \tag{3}$$

substituting equation (2) into (3) gives

$$v_i = i_2 (s^2 L_2 C + 1) \left(sL_1 + \frac{sL_2}{s^2 L_2 C + 1} \right) \tag{4}$$

hence, the transfer function

$$H_{(S)} = \left({}^{i_2(s)}\!/_{v_i(s)} \right) = \frac{1}{s^3 (L_1 L_2 C) + s(L_1 + L_2)} \tag{5}$$

is obtained from equation (4)

or

$$H_{(S)} = \left({}^{i_2(s)}\!/_{v_i(s)} \right) = \frac{1}{s(L_1 L_2 C)} \bullet \frac{1}{s^2 + \omega_r^2} \tag{6}$$

where $\omega_r = \sqrt{\dfrac{L_1 + L_2}{L_1 L_2 C}}$ *and* $f_r = {}^{\omega_r}\!/_{2\pi}$

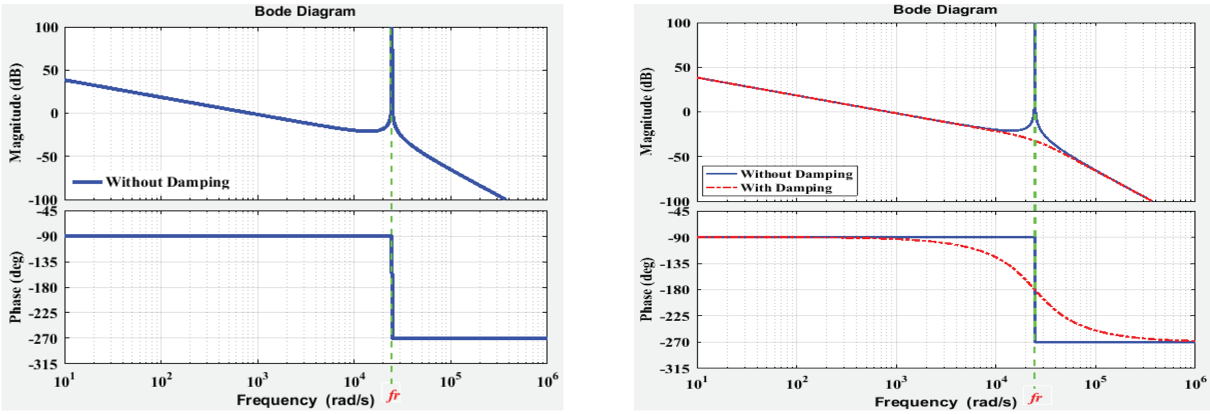

(a) without damping term (b) With damping

Figure 2: BD of LCL filter

The sharp step down of -180^o at the oscillatory frequency is caused by the LCL smoother oscillation and has a high resonance peak magnitude. This may lead to system instability from control perspective [11], since -180^o is a negative crossing, it will generate a plane poles with a pair of closed-loop right-half. By damping the resonance below $0dB$ negative crossing is avoided. The damping ratio ζ which is a first order term related to s is infused in the oscillatory term $s^2+\omega_r^2$ of equation (6) to obtain

$$H_{damp(S)} = \left(i_2(s) \big/ v_i(s) \right) = \frac{1}{s(L_1L_2C)} \bullet \frac{1}{s^2+2s\zeta\omega_r+\omega_r^2} \quad (7)$$

The dashed lines in Fig. 2(b) is the plot of the $H_{damp(S)}$. By introducing the damping term, shows that the magnitude and frequency characteristic resonance remain unchanged but the oscillatory peak of the smoother is effectively reduced.

3.0 CHARACTERISTIC DISGN OF DIFFERENT DAMPING CONFIGURATION

The damping solutions to suppress the resonance problems of the LCL filter are given in this section. Six damping solution exist, according to the location of the damping term. Detailed analyses of the solution are presented as follows;

A. Case 1: R - L₁ Series Connection

$$H_{R_{1s}(S)} = \left(i_2(s) \big/ v_i(s) \right) = \frac{1}{s^3(L_1L_2C)+s^2L_2CR_{1s}+s(L_1+L_2)+R_{1s}} \quad (8)$$

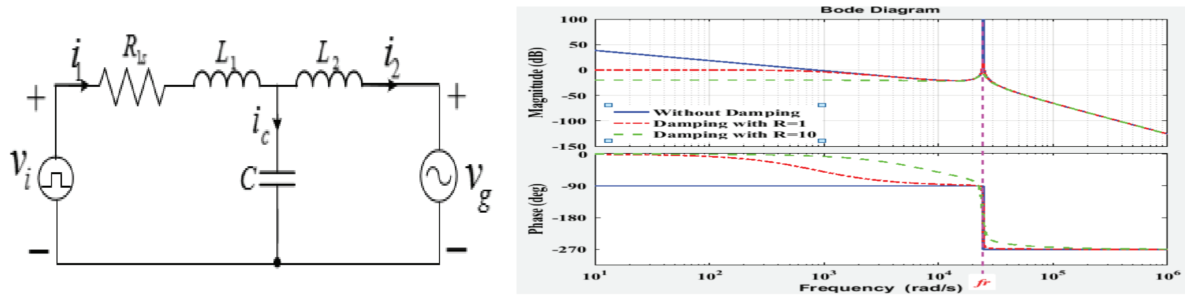

(a) *(b)*

Figure 3: (a) Resistor R_{1s} connected in series with Inductor L_1. (b) BD of the transfer function.

B. Case 2: R - L_2 Series Connection

$$H_{R2s(S)} = \left(i_2(s) \big/ v_i(s) \right) = \frac{1}{s^3(L_1L_2C)+s^2L_1CR_{2s}+s(L_1+L_2)+R_{2s}} \tag{9}$$

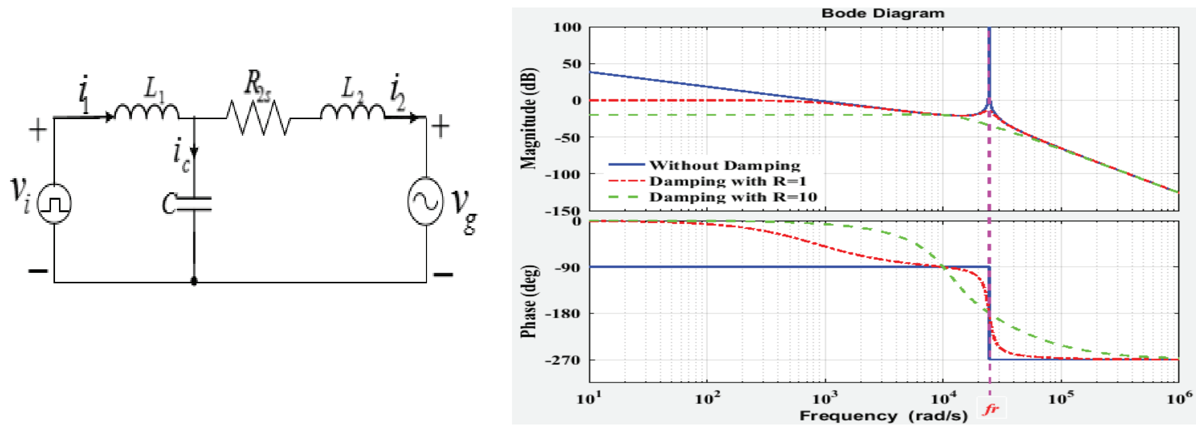

(a) *(b)*

Figure 4: (a) Resistor R_{2s} connected in series with Inductor L_2. (b) BD of the transfer function

C. Case 3: R - L_1 Shunt Connection

$$H_{R_{1p}(S)} = \left(i_2(s) \big/ v_i(s) \right) = \frac{sL_2/R_{1p}+1}{s^3(L_1L_2C)+\frac{s^2L_1L_2}{R_{1p}}+s(L_1+L_2)} \tag{10}$$

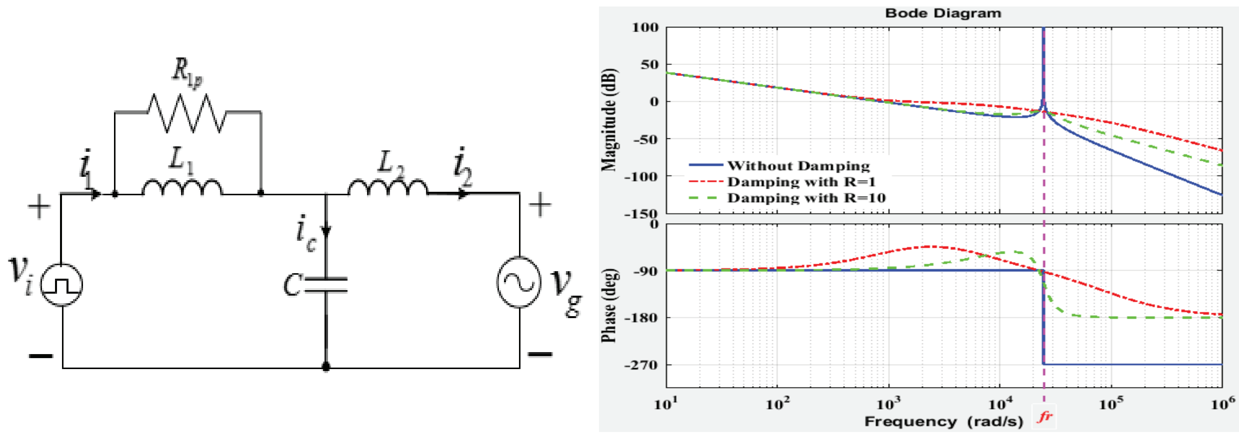

(a) *(b)*

Figure 5: (a) Resistor R_{1p} ***connected in parallel with Inductor*** L_1***. (b) BD of the transfer function***

D. Case 4: R - L_2 Shunt Connection

$$H_{R_{2p}(S)} = \left(i_2(s) \Big/ v_i(s) \right) = \frac{sL_2/R_{2p} + 1}{s^3(L_1L_2C) + \dfrac{s^2 L_1 L_2}{R_{2p}} + s(L_1 + L_2)} \tag{11}$$

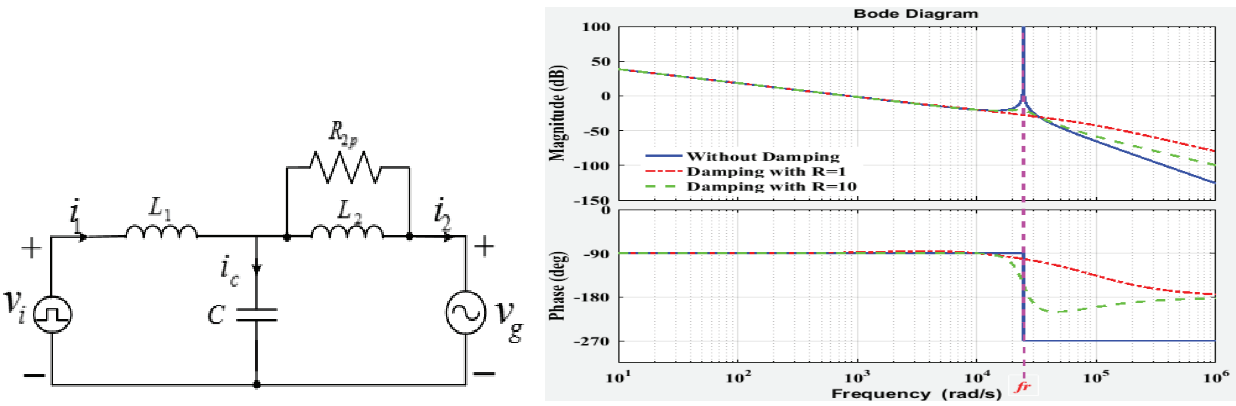

(a) *(b)*

Fig.6: (a) Resistor R_{2p} ***connected in parallel with Inductor*** L_2***. (b) BD of the transfer function***

E. Case 5: C - R Series Connection

$$H_{R_{cs}(S)} = \left(i_2(s) \Big/ v_i(s) \right) = \frac{sR_{cs}C + 1}{s^3(L_1L_2C) + s^2 R_{cs} C(L_1 + L_2) + s(L_1 + L_2)} \tag{12}$$

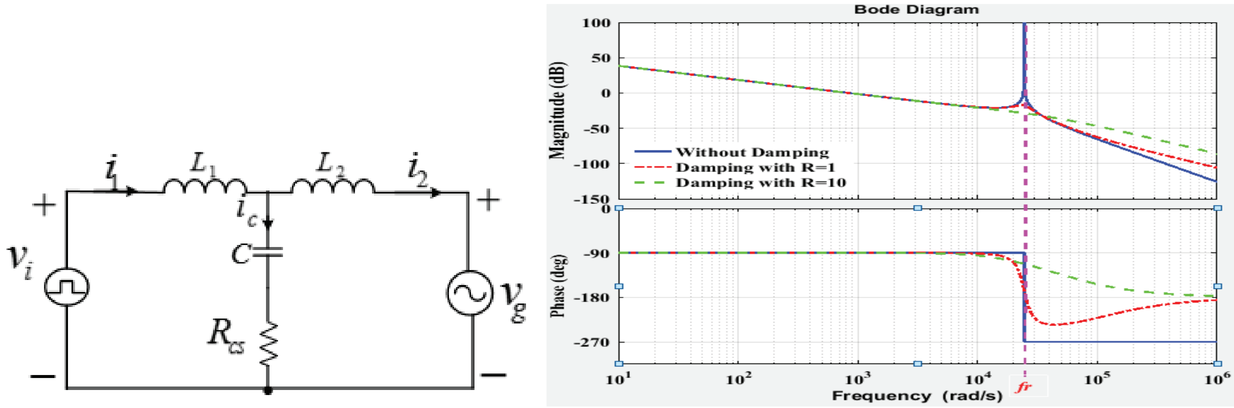

(a) *(b)*

Figure 7: (a) Resistor R_{cs} connected in series with Capacitor,C (b) BD of the transfer function

F. Case 6: C - R Shunt Connection

$$H_{R_{cp}(S)} = \left({i_2(s)} \middle/ {v_i(s)} \right) = \frac{1}{s^3 (L_1 L_2 C) + \frac{s^2 L_1 L_2}{R_{cp}} + s(L_1 + L_2)} \qquad (13)$$

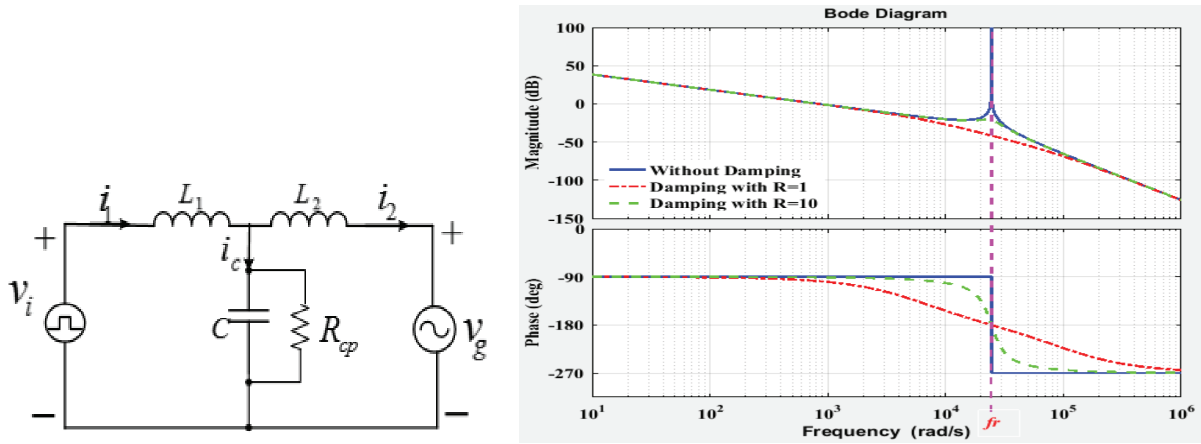

(a) *(b)*

Figure 8: (a) Resistor R_{cp} connected in parallel with Capacitor C. (b) BD of the transfer function

It can be observed from the six different damping cases that, similar transfer functions from v_i *to* i_2 are obtained when a series resistor is connected to inductors, L_1 *and* L_2. Thus, by comparing equations (8) and (9), a second-order term related to s (damping factor) as well as a constant term are added to the divisor of the transfer function $H_{(s)}$. Similarly, the transfer functions of equations (10), (11) and (12) are similar when the resistor is placed in parallel to inductors L_1 *and* L_2 respectively and/or place in series with the capacitor C. Beside the introduction of a damping term as seen, a zero is also added. Finally, equation (13) is similar to (7) with only damping term being added to the denominator.

The Bode diagram of the transfer functions of equation (8) and (9) are shown in Figures 3(b) and 4(b) respectively, where it is interesting to note that, resistor placed in series with L_1 *and* L_2 reduces the low frequency gain of the LCL smoother. This is because the impedance of the inductor branch depends on the resistor value at low frequency spectrum. This means that the higher the value of the resistor the lower the frequency gain at the low frequency range. However, at the high frequency range, the impedance depends on the reactive inductance, which means that the resistor has no effect on the LCL filter at high frequency range.

On the contrary, from Figures 5(b) and 6(b), it can be observed that the high frequency gain is increased, thereby weakening the attenuation capability of the LCL at the high frequency spectrum. This is because, even though the reactive inductance is comparatively large, the resistor connect in shunt minimizes the total impedance. In the lower frequency spectrum, the inductive reactance value is greater than the resistance and therefore does not affect the frequency gain.

Figure 7 (b) looks like that of Figures 5(b) and 6(b), where we can observe that the harmonic attenuation ability is weak in the high frequency spectrum as a result of additional series resistor connected with the capacitor. This is because capacitive reactance is relatively large at high frequency. Hence, the impedance depends on the resistor value and poor harmonic attenuation will be experienced if the resistance is increased. At the high frequency ranges, the resistor has no effect on the frequency gain.

Finally, from Figure 8 (b), it can be seen that the magnitude and frequency high and low frequency spectrum are not affected by the parallel resistor connected to the capacitor. These six cases were incorporated into a three-phase system to ascertain their dynamic characteristics.

4.0 SIMULATION RESULTS

The performance of the above analysis was verified by simulating using an equivalent three-phase system of Figure 1: (a) with MATLAB-Simulink tools. The parameters listed in Table 1 were used. The operating principles of the APF control circuit is in accordance with the instantaneous power theory [13]. The phase locked loop (PLL) which ought to be in phase with the compensation current is used to generate cosine and sine signal $(\sin\omega t \text{ and } \cos\omega t)$. The Clark transformation matches the three-phase instantaneous line current in (a,b,c) into two-phase instantaneous current (α,β). A pulse width modulation (PWM) with switching frequency of $10kHz$ was used to generate the switching signals for the voltage source inverter (VSI). Figures (10-15) show the system performance of the six different damping cases of the LCL filter after compensation in terms of waveforms and the FFT analysis of the grid current.

Table 1: Simulation parameters

Parameter	Value
P_r (Rated power)	$6kW$
V_{LL} (Line-Line Voltage)	$220V$
F_g (Grid frequency)	$50Hz$
F_{sw} (Switching frequency)	$10kHz$
V_{dc} (DC link Voltage)	$360V$
Selected LCL Filter Value	
L_1	$1mH$
L_2	$0.2mH$
C	$10\mu F$

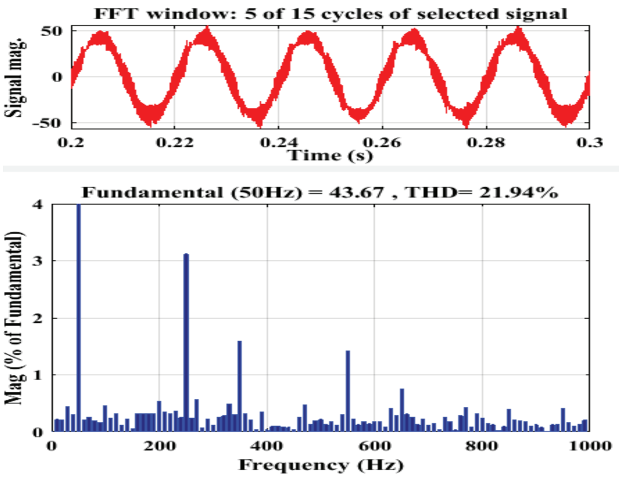

Figure 10: Waveform and FFT analysis of damping resistor in series with L_1

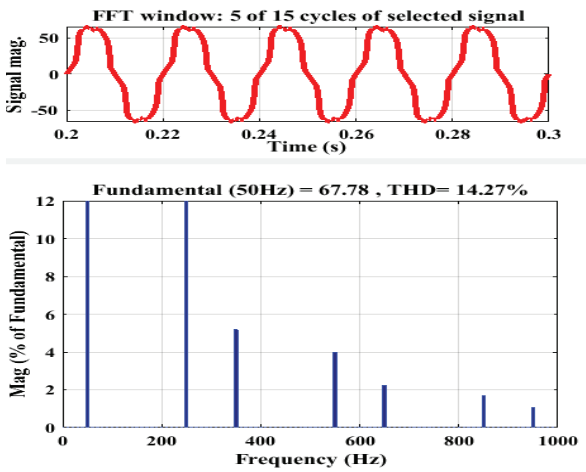

Figure11: Waveform and FFT analysis of damping resistor in series with L_2

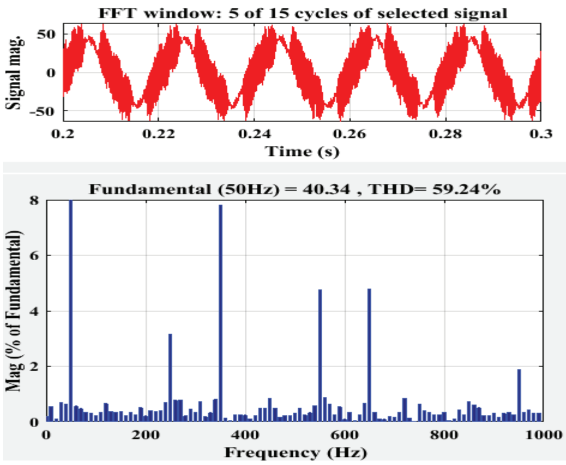

Figure 12: Waveform and FFT analysis of damping resistor in parallel with L_1

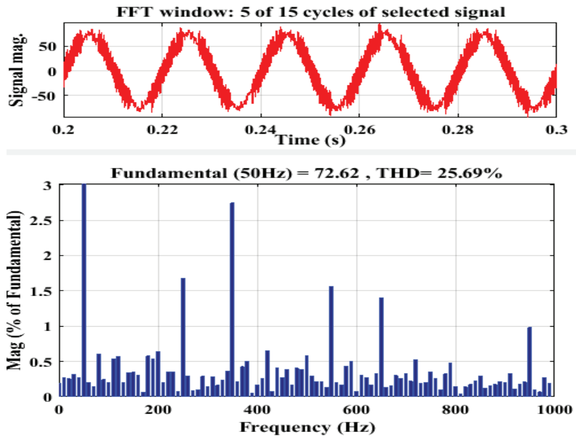

Figure 13: Waveform and FFT analysis of damping resistor in parallel with L_2

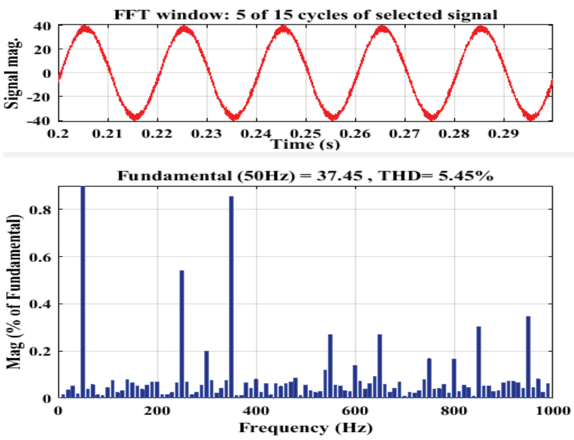

Figure 14: Waveform and FFT analysis of series resistor-capacitor damping technique

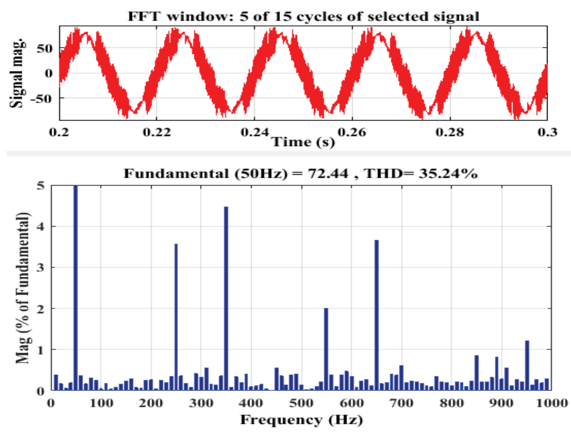

Figure 15: Waveform and FFT analysis of shunt resistor-capacitor damping technique

In light of above analysis, it can be observed from the Bode diagrams that placing a shunt resistor with the smoother capacitor C is paramount among the six passive damping remedies. Notwithstanding, the simulation results show that, it is not applicable in practice because of its high power losses. This is because the capacitor voltage is directly applied to the parallel resistor. Hence, series resistor-capacitor is the best passive damping methods for real time application, since it has the lowest THD.

5.0 CONCLUSION

This paper has presented a step by step analysis of the various oscillatory damping techniques of an LCL smoother. Passive damping technique for the output LCL smoother of an inverter used in APF harmonic compensation was discussed. The Bode diagrams of the various passive damping methods were analyzed. MATLAB-Simulink was used to verify the damping method and it has shown that placing a damping term parallel to the filter capacitor show it real impracticability even though the Bode diagram shows that it has better resonance attenuation compared to the other method. However, it has shown that placing series resistor with the capacitor C gives,in terms low THD and low power loss, the best performance .

REFERENCES

J. Zhang, Z. Zhang, and Y. Huang, “An Improved Decoupling Control Scheme for Active Power Filter Compensators,” in IEEE Transactions on Industrial Electronics, vol. 68, no. 2, pp. 1137-1147, Feb. 2021.

M. M. El-Zahab, H. M. Fahmy, and M. A. Abido, “Enhanced Active Power Filter Compensator for Harmonic Mitigation Based on Hybrid Optimization Algorithm,” in IEEE Transactions on Industrial Electronics, vol. 68, no. 9, pp. 7977-7987, Sep. 2021.

A. Hussain, M. Islam, and S. Mekhilef, “Adaptive Control Algorithm for Active Power Filter Compensators in Nonlinear Loads,” in IEEE Transactions on Industrial Informatics, vol. 17, no. 1, pp. 297-306, Jan. 2021.

K. Srinivas and D. K. Mohanta, “An Adaptive Neuro-Fuzzy Inference System-Based Hybrid Control Approach for Active Power Filter Compensators,” in IEEE Transactions on Industrial Electronics, vol. 68, no. 5, pp. 4247-4256, May 2021.

S. Bouktir, M. Ouhrouche, and B. François, “An Adaptive Predictive Control Algorithm for Active Power Filter Compensators,” in IEEE Transactions on Industrial Electronics, vol. 68, no. 8, pp. 6492-6501, Aug. 2021.

C. L. Naik, A. Chandra, and B. Singh, “Modified Intelligent Control for Active Power Filter Compensators,” in IEEE Transactions on Industry Applications, vol. 57, no. 5, pp. 5636-5646, Sep./Oct. 2021.

J. Wang, J. Yang, and B. Zhang, “Design of LCL Filters for Grid-Connected Inverters Based on Small-Signal Modeling and Load Resilience,” IEEE Transactions on Power Electronics, vol. 36, no. 7, pp. 7838-7849, Jul. 2021.

S. Liu, J. Qin, Y. Zhang, and Y. Liu, “Design and Analysis of LCL Filters with Reduced DC-Link Capacitance for Grid-Tied Inverters,” IEEE Transactions on Industrial Electronics, vol. 68, no. 6, pp. 5003-5014, Jun. 2021.

Y. Chen, X. Liu, W. Xiang, and Y. Wu, “Modeling and Control of LCL Filters in Grid-Connected Inverter Systems under Unbalanced Grid Voltage Conditions,” IEEE Transactions on Power Electronics, vol. 36, no. 3, pp. 3561-3573, Mar. 2021.

Goodwin, G.C., Graebe, S.F., Salgado, M.E.: Control System Design. Prentice Hall, Upper Saddle River, NJ (2000)

H. A. Salama, S. J. Finney, and B. W. Williams, “Predictive Control of LCL Filters for Grid-Connected Inverters,” IEEE Transactions on Industrial Electronics, vol. 68, no. 3, pp. 2192-2202, Mar. 2021.

M. Marcu, F.-G. Popescu, T. Niculescu, L. Pana, and A. D. Handra, “Simulation of power active filter using instantaneous reactive power theory,” in *Proceedings of the 16th*

International Conference on Harmonics and Quality of Power (ICHQP '14), pp. 581–585, Bucharest, Romania, May 2014.

A. Patra, K. K. Sen, and A. K. Pradhan, "Improved Design of LCL Filters for Grid-Connected Inverters," IEEE Transactions on Power Electronics, vol. 36, no. 2, pp. 1976-1989, Feb. 2021.